10.1109/ULTSYM.2010.0346

Monitoring Radiofrequency Catheter Ablation using Thermal Strain Imaging

Chi Hyung Seo[1], Douglas Stephens[2], Jonathan Cannata[3], Aaron Dentinger[4], Feng Lin[4], Suhyun Park[4], Douglas Wildes[4], Kai Thomenius[4], Peter Chen[5], Tho Nguyen[5], Alan Delarama[5], Jong Seob Jeong[3], Aman Mahajan[6], Kalyanam Shivkumar[6], Omer Oralkan[7], David Sahn[8], Pierre Khuri-Yakub[7], Matthew O'Donnell[1]

[1]University of Washington, USA, [2]University of California, Davis, USA, [3]University of Southern California, USA, [4]GE Global Research, USA, [5]St. Jude Medical, USA, [6]David Geffen School of Medicine at UCLA, USA, [7]Stanford University, USA, [8]Oregon Health and Science University, USA

Abstract— **A method to monitor ablative therapy by examining slope changes in the thermal strain curve caused by speed of sound with temperature is introduced. The variation of sound speed with temperature rise for most soft tissue follows a similar pattern to that of water. Unlike most liquids, the sound speed of tissue increases with temperature. However, at temperatures above about 50 °C, there is no further increase in the sound speed and the temperature coefficient may become slightly negative. For ablation therapy, an irreversible injury to tissue and a complete heart block occurs in the range of 48 – 50 °C for a short period in accordance with the well known Arrhenius equation. Using these two properties, we propose a potential tool to detect the moment when tissue damage occurs using the reduced slope in the thermal strain curve as a function of heating time. Using a prototype intracardiac echocardiography (ICE) array for imaging and a catheter for RF ablation, we were able to observe an obvious slope change in the thermal strain curve in an excised tissue sample. The method was further tested in-vivo, using a specially equipped ablation tip and an 11 MHz microlinear (ML) ICE array mounted on the tip of a catheter. As with in-vitro experiments, the thermal strain curve showed a plateau and a change in the sign of the slope.**

I. Introduction

Catheter ablation has become a significant modality to manage cardiac arrhythmias [1]-[3]. It has transformed the field of cardiac electrophysiology from a diagnostic tool to a potent prophylactic and curative method. An exciting recent development is the increasing adoption of catheter ablation for atrial fibrillation [4]. Atrial fibrillation is the most frequent arrhythmia in clinical practice and its incidence is increasing as the population ages [5].

Radio frequency ablation (RFA) is used in electrophysiology (EP) procedures to permanently alter the myocardium in locations which support aberrant electrical conduction pathways contributing to irregular heart rhythm. Tissue temperature is critically related to the success or failure of catheter ablation procedures [6], [7]. To ensure irreversible injury, a tissue temperature of approximately 50 °C must be achieved [6], [7]. The minimum temperature needed to create a complete heart block has been observed to be 48 °C [8], [9]. Raising tissue temperature significantly beyond this point can be unnecessary and can cause complications during the procedure. High temperature at the tissue site may result in coagulum formation on the electrode, endocardial disruption, steam popping, or perforation. This would lead to an abrupt rise in electrical impedance which would result in a marked decrease in tissue heating [10], [11]. Furthermore, if a coagulum develops, the ablation catheter must be removed, cleaned, and repositioned, necessitating additional catheter manipulation and additional fluoroscopy time.

Funding is provided by the NIH/NHLBI R01-HL67647, USA

The signal-processing methods proposed in this paper were developed to investigate the feasibility of monitoring ablative therapy for the myocardium by identifying the point at which the slope of the thermal strain curve changes sign caused by speed of sound and thermal expansion variations with temperature. First, a dynamic heating experiment is performed using excised bovine tissue *in-vitro*. The feasibility of our method of temperature monitoring is tested *in-vivo*.

II. Methods

A. Dynamic heating experiment in-vitro

To ensure that sufficient heat could be delivered for lesion formation, excised beef muscle was prepared in a saline solution. Beef muscle instead of a porcine heart was used for this initial in-vitro experiment, since both are water-bearing tissue with a similar sound speed versus temperature profile. The dimensions of the sample were 20 cm × 10 cm with a 2 cm thickness. While under water, the sample was fixed on a holder to minimize any motion. It was then allowed to reach 37 ºC (about 2 hours) in a heated saline bath before the experiment began.

RF data was collected using a prototype side-looking HockeyStick (HS) ICE catheter array [12] interfaced with the GE Vivid 7 imaging system while RF ablation was driven by a Stockert RF generator (Biosense Webster, Inc, Diamond Bar, California) with a Biosense-Webster dual-sensor 8mm catheter. The ultrasound transmit frequency was 10 MHz with a transmit focus at 15 mm. Temperatures in the tissue were measured using an implanted fine wire thermocouple. Thermocouple, ablation catheter, and HS array were positioned as in Figure 1. A digital thermocouple reader was used to record the temperature at 1 second intervals.

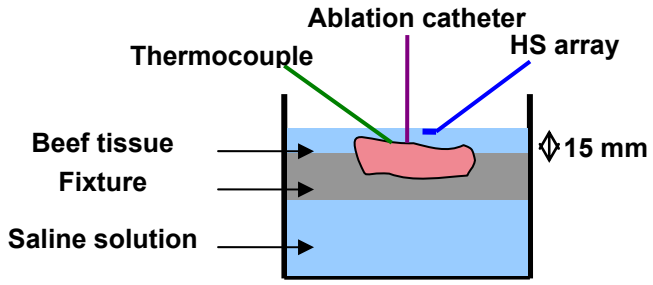

Figure 1. Diagram showing relative positions of the thermocouple, ablation catheter, and HS array in dynamic *in-vitro* heating experiment.

B. Catheter ablation experiment in-vivo

For an in-vivo study, juvenile Yorkshire pigs were used as the animal model. All surgical methods and animal treatment procedures used were approved by the Animal Care and Use Committees of the University of California, Los Angeles. All animals were given general anesthesia and were maintained with 2 % isoflurane and oxygen ventilation. Femoral arteries and veins as well as jugular veins were exposed by surgical incision ready for catheter access. Electrocardiograms, body temperature, and oxygen saturation were continuously monitored. Electrocardiography (ECG) electrodes were connected to the body of the pig for standard three point recording. The output of the ECG served as the trigger for the Irvine Biomedical Inc. (IBI) generator (St. Jude Medical, Inc, St. Paul, Minnesota). The generator was active for 300 ms beginning at the peak of the ECG "R" wave, then inactive until the next trigger. The respirator was stopped during data acquisition (20 seconds) to reduce undesired motion such that the dominant physiological motion would be heart motion.

We used a specially designed ultrasound compatible radiofrequency ablation tip integrated into a prototype 9F forward-looking microlinear (ML) ICE catheter array to simultaneously image and ablate the right atrial wall [13]. The transmit frequency was 11 MHz with a transmit focus at 5 mm. Ablation was performed while the integrated imaging and ablation catheter was localized and guided by fluoroscopy and EnSite NavX™ Navigation & Visualization Technology (St. Jude Medical, Inc, St. Paul, Minnesota) [12].

Continuous ultrasound data was acquired during ablation. Noise from the RF generator did not diminish B-mode image quality.

C. TSI Signal Processing

Since ultrasound data acquisition was not triggered by the ECG, we assumed that the heart returns to its initial state before ablation.

Four frames of data with the least motion were selected by examining B-mode images from the first cardiac cycle before ablation. Using these as reference frames, 2-D cross-correlation was performed to find the best matched frame with the highest cross-correlation (>=0.85) within a cycle for all subsequent cardiac phases. Then, using each frame from the first cardiac cycle as a reference, 2-D speckle tracking was performed with all corresponding frames throughout the experiment. These four displacement sets were averaged to produce the measured axial displacement (Figure 2).

Two-dimensional phase-sensitive correlation-based speckle tracking [14] was applied to RF data from every frame in the sequence to estimate temporal strain along the axial direction. The tracking algorithm involves calculating complex cross-correlation coefficients between small windowed blocks from two consecutive frames, reducing the probability of peak hopping by filtering the correlation coefficient functions, and estimating the shift from the phase zero-crossing around the peak correlation coefficient. The correlation kernel size was about the full-width-half-maximum (FWHM) of a speckle autocorrelation function for optimal strain estimation. Reduced kernel size and correlation filtering significantly decreases peak hopping probability and increases the accuracy of displacement estimation [14].

Axial displacement was estimated from the position of the maximum correlation coefficient, and was further refined using the phase zero-crossing of the complex correlation function. The kernel size used for tracking in-vivo was slightly larger than the speckle size, approximately 0.3 mm × 6.6 ° (axial × lateral) and the filter size was 0.75 mm × 7.3 ° (axial × lateral). Spatial derivatives of the displacements were computed to estimate temporal strain due to the sound speed change from axial displacement using a simple 1-D difference filter along the axial direction for correlation windows separated by 0.9 mm.

III. RESULTS

A. Dynamic heating experiment in-vitro

Figure 3 plots the thermal strain against the temperature rise. The region used to produce the plot is highlighted. Several representative pixels in the focal region were averaged to plot thermal strains. The region averaged for this plot is also shown in the figure. Here, there is an obvious sign change in the slope of the thermal strain curve at around 50 °C. By plotting the slope of the thermal strain curve as a function of temperature, we can also observe this sign change at around 50 °C (Figure 4). Figure 5 is the photograph of the visible lesion formed from RF ablation.

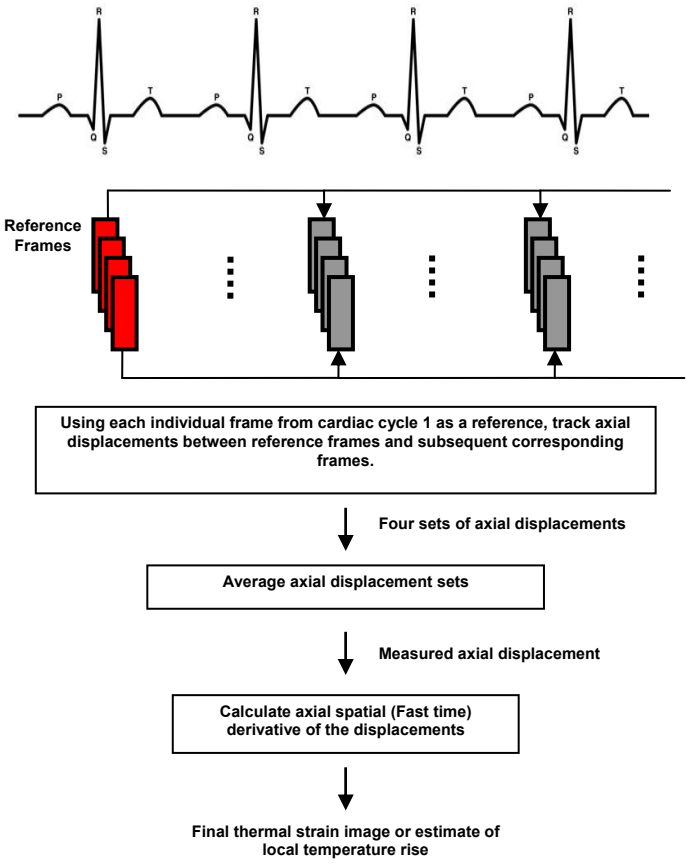

Figure 2. Block diagram describing processing steps to generate thermal strain image.

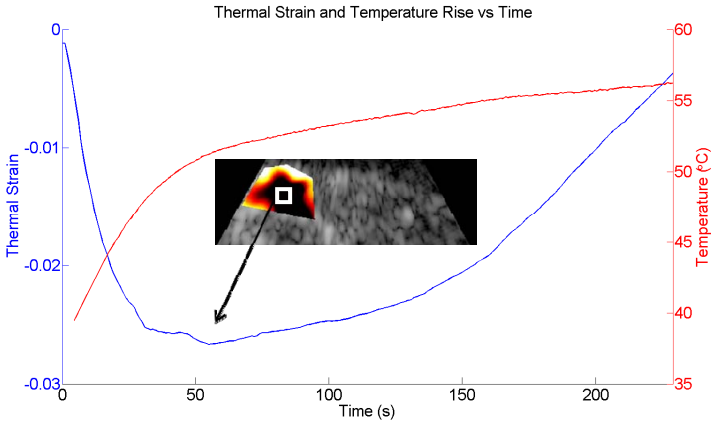

Figure 3. Thermal strain plotted with temperature rise in beef tissue using a HS array.

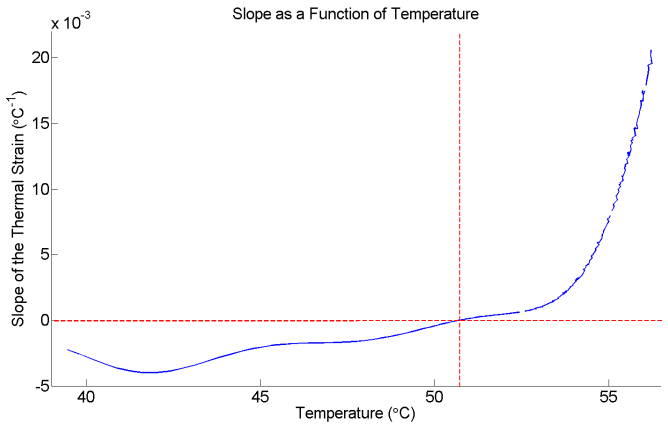

Figure 4. The slope of the fitted thermal strain curve in Figure 3 plotted as a function of temperature.

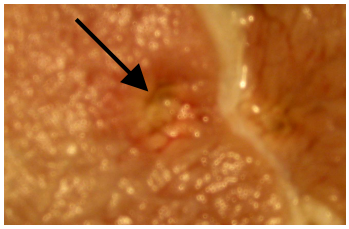

Figure 5. Lesion formed after RF ablation.

B. Catheter ablation experiment in-vivo

Figure 6 plots the thermal strain vs time. Several representative pixels in the highlighted region were averaged to plot the thermal strains. Similar to the in-vitro case, there is a sign change at around 12 seconds. Since there was no direct temperature measurement, we have estimated the temperature rise using finite element modeling. Using thermal strain, it is clear when the temperature reaches at least 50 °C. Figure 7 shows the lesions formed by RF ablation.

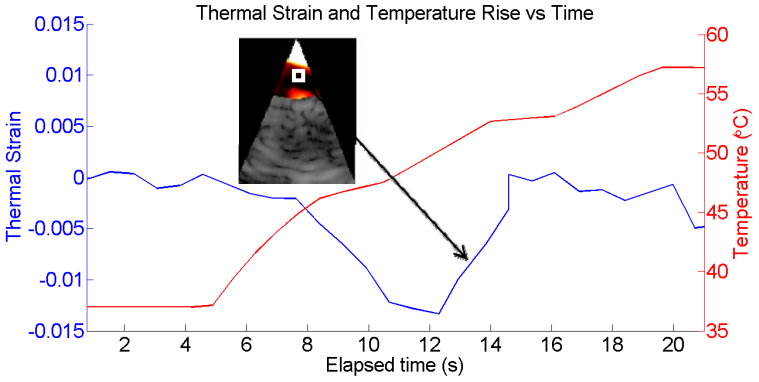

Figure 6. Thermal strain plot is generated using representative pixels. The temperature rise was estimated from finite element modeling.

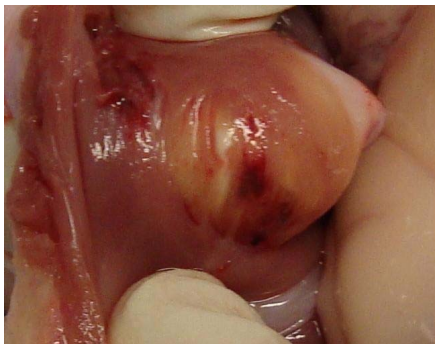

Figure 7. Lesion formed by RF ablation on the right atrial wall.

IV. DISCUSSION AND FUTURE WORK

The potential of monitoring temperature during RF ablation using a slope change in the thermal strain curve has been demonstrated. For both *in-vitro* and *in-vivo* experiments, thermal strain curves showed a plateau then slope change at around 50 °C. Although only a single *in-vivo* experiment is reported here and additional *in-vivo* studies need to be performed to better evaluate the robustness of this technique, preliminary results are promising.

REFERENCES

[1] W. M. Jackman, X. Wang, K. J. Friday, C. A. Roman, K. P. Moulton, K. J. Beckman, J. H. McClelland, N. Twidale, H. A. Hazlitt, M. I. Prior, P. D. Margolis, J. D. Calame, E. D. Overholt, and R. Lazzara, "Catheter ablation of accessory atrioventricular pathways (Wolff-Parkinson-White Syndrome) by radiofrequency current," N Eng J Med 1991; 324: 1605-1611.

[2] H. Calkins, E. Prystowsky, M. Carlson, L. S. Klein, J. P. Saul, and P. Gillette, "Temperature monitoring during radiofrequency catheter ablation procedures using closed loop control," Circulation 1994; 90:1279-1286.

[3] M. D. Lesh, G. F. Van Hare, D. J. Schamp, W. Chien, M. A. Lee, J. C. Griffin, J. J. Langberg, T. J. Cohen, K. G. Lurie, and M. M. Scheinman, "Curative percutaneous catheter ablation using radiofrequency energy for accessory pathways in all locations: Results in 100 consecutive patients," J Am Coll Cardiol 1992; 19:1303-1309.

[4] L. M. Epstein, N. Chiesa, M. N. Wong, R. J. Lee, J. C. Griffin, M. M. Scheinman, and M. D. Lesh, "Radiofrequency catheter ablation in the treatment of supraventricular tachycardia in the elderly," J Am Coll Cardiol 1994; 23:1356-1362.

[5] N. S. Peters, R. J. Schilling, and P. Kangaratnam, and V. Markides, "Atrial fibrillation: strategies to control, combat, and cure," Lancet, 359:593-603.

[6] S. Nath, C. Lynch, J. G. Whayne, and D. E. Haines, "Cellular electrophysiologic effects of hyperthermia on isolated guinea pig papillary muscle: implications for catheter ablation," Circulation 1993; 88:1826-1831.

[7] D. E. Haines and D. D. Watson, "Tissue heating during radiofrequency catheter ablation: a thermodynamic model and observations in isolated perfused and superfused canine right ventricular free wall," PACE Pacing Clin Electrophysiol. 1989; 12:962-976.

[8] J. J. Langberg, H. Calkins, R. el-Atassi, M. Borganelli, A. Leon, S. J. Kalbfleisch, and F. Morady, "Temperature monitoring during radiofrequency catheter ablation of accessory pathways," Circulation 1992; 86;1469-1474.

[9] R. H. Falk, "Atrial Fibrillation," N Engl J Med, vol. 344, no. 14 April 5, 2001.

[10] D. E. Haines and A. F. Verow, "Observations on electrode-tissue interface temperature and effect on electrical impedance during radiofrequency ablation of ventricular myocardium," Circulation. 1990; 82:1034-1038.

[11] G. Hindricks, W. Haverkamp, H. Gulker, U. Rissel, T. Budde, K. D. Richter, M. Borggrefe, and G. Breithardt, "Radiofrequency coagulation of ventricular myocardium: improved prediction of lesion size by monitoring catheter tip temperature," Eur. Heart J., vol. 10, pp. 972-984, 1989.

[12] D. N. Stephens, J. Cannata, R. Liu, J. Z. Zhao, K. K. Shung, H. Nguyen, R. Chia, A. Dentinger, D. Wildes, K. E. Thomenius, A. Mahajan, K. Shivkumar, K. Kim, M. O'Donnell, A. Nikoozadeh, O. Oralkan, P. T. Khuri-Yakub, and D. J. Sahn, "Multifunctional Catheters Combining Intracardiac Ultrasound Imaging and Electrophysiology Sensing," IEEE Trans. Ultrason., Ferroelect., Freq. Contr., vol. 55, pp. 1570–1581, 2008.

[13] D. N. Stephens, M. O'Donnell, K. E. Thomenius, A. Dentinger, D. Wildes, P. Chen, K. K. Shung, J. Cannata, P. T. Khuri-Yakub, O. Oralkan, A. Mahajan, K. Shivkumar, and D. J. Sahn, "Experimental Studies With a 9F Forward-Looking Intracardiac Imaging and Ablation Catheter", J Ultrasound Med. 2009; 28:207–215.

[14] M. A. Lubinski, S. Y. Emelianov, and M.O'Donnell, "Speckle tracking methods for ultrasonic elasticity imaging using short time correlation," IEEE Trans. Ultrason., Ferroelect., Freq. Contr., vol. 46, pp. 82–96, 1999.